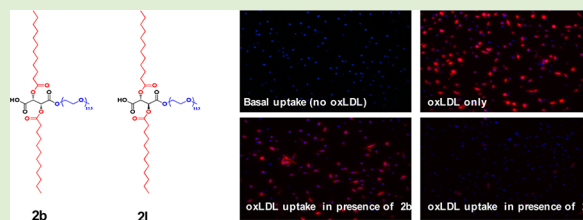


Nanoscale Amphiphilic Macromolecules with Variable Lipophilicity and Stereochemistry Modulate Inhibition of Oxidized Low-Density Lipoprotein Uptake

Dawanne E. Poree,[†] Kyle Zablocki,[‡] Allison Faig,[†] Prabhas V. Moghe,^{‡,§} and Kathryn E. Uhrich^{*,†}

[†]Departments of Chemistry and Chemical Biology, [‡]Biomedical Engineering, and [§]Chemical and Biochemical Engineering, Rutgers University, Piscataway, New Jersey 08854, United States

ABSTRACT: Amphiphilic macromolecules (AMs) based on carbohydrate domains functionalized with poly(ethylene glycol) can inhibit the uptake of oxidized low density lipoprotein (oxLDL) and counteract foam cell formation, a key characteristic of early atherogenesis. To investigate the influence of lipophilicity and stereochemistry on the AMs' physicochemical and biological properties, mucic acid-based AMs bearing four aliphatic chains (2a) and tartaric acid-based AMs bearing two (2b and 2l) and four aliphatic chains (2g and 2k) were synthesized and evaluated. Solution aggregation studies suggested that both the number of hydrophobic arms and the length of the hydrophobic domain impact AM micelle sizes, whereas stereochemistry impacts micelle stability. 2l, the meso analogue of 2b, elicited the highest reported oxLDL uptake inhibition values (89%), highlighting the crucial effect of stereochemistry on biological properties. This study suggests that stereochemistry plays a critical role in modulating oxLDL uptake and must be considered when designing biomaterials for potential cardiovascular therapies.



I. INTRODUCTION

Atherosclerosis, a disease characterized by occlusion of the arteries, is triggered by the build-up of oxidized low density lipoprotein (oxLDL) in vascular intima.¹ The oxLDL accumulation generates an inflammatory response, resulting in the recruitment of circulating monocytes, followed by their differentiation into macrophages, resulting in the upregulation of macrophage scavenger receptors.² The uptake of oxLDL is mediated by these scavenger receptors, namely scavenger receptor A (SR-A) and cluster of differentiation 36 (CD36),^{3–5} leading to unregulated cholesterol accumulation and foam cell formation, a key characteristic of the onset of atherogenesis.^{6,7}

To date, cholesterol-lowering therapies (i.e., statins) are the most common methods for management of the long-term effects of atherosclerosis. These drugs indirectly ameliorate the cascade of atherosclerosis by decreasing cholesterol synthesis; however, the ultimate impact on the deposition of oxLDL in the blood vessel walls has not been clearly established. A more direct and promising approach in the treatment and prevention of atherosclerosis involves designing functional inhibitors against scavenger receptors to abrogate uncontrolled oxLDL uptake.^{8–11} Our research group has previously prepared nanoscale amphiphilic macromolecules (AMs) capable of inhibiting oxLDL uptake through competitive inhibition of SR-A and CD36 scavenger receptors in IC21 macrophage cells.¹² Comprised of a mucic acid backbone, four aliphatic chains, and a poly(ethylene glycol) (PEG) tail, these biocompatible AMs (2a, Figure 1a) form nanoscale micelles in aqueous media at relatively low critical micelle concentrations (10^{-7} M).¹³ To determine the key structural components critical for oxLDL uptake inhibition, this AM

structure has been systematically varied to determine the role of PEG chain length and architecture, carboxylic acid location, type and number of anionic charges, and rotational motion of the anionic group.¹⁴ The role that comparative hydrophobicity and stereochemistry play in inhibiting oxLDL uptake, however, has not been actively explored. Based on previous molecular modeling and experimental studies, the hydrophobic domain of these AMs appears to be actively involved in binding to macrophage scavenger receptors.¹⁵ These previous studies correlate well with literature that suggests that hydrophobic interactions play a major role in protein–polymer complexation.^{16–18}

As a preliminary study to probe the effect of lipophilicity on the polymer's physicochemical and biological properties, our research group compared 2a to an analogous AM comprised of an L-tartaric acid (L-TA) backbone bearing only two aliphatic chains (2b, Figure 1a). Investigating the physicochemical properties of these two AMs showed that an increase in lipophilicity rendered more stable micelles, as determined by the critical micelle concentration (CMC, a measure of solution stability), with larger hydrodynamic radii. To investigate the impact of lipophilicity on their biological properties, these AMs were tested for their ability to inhibit oxLDL uptake in peripheral blood mononuclear cells (PBMCs) under serum-free conditions. While both polymers inhibited oxLDL uptake in PBMCs compared to 35% inhibition achieved by 2b (Figure

Received: April 16, 2013

Revised: June 18, 2013

Published: June 24, 2013

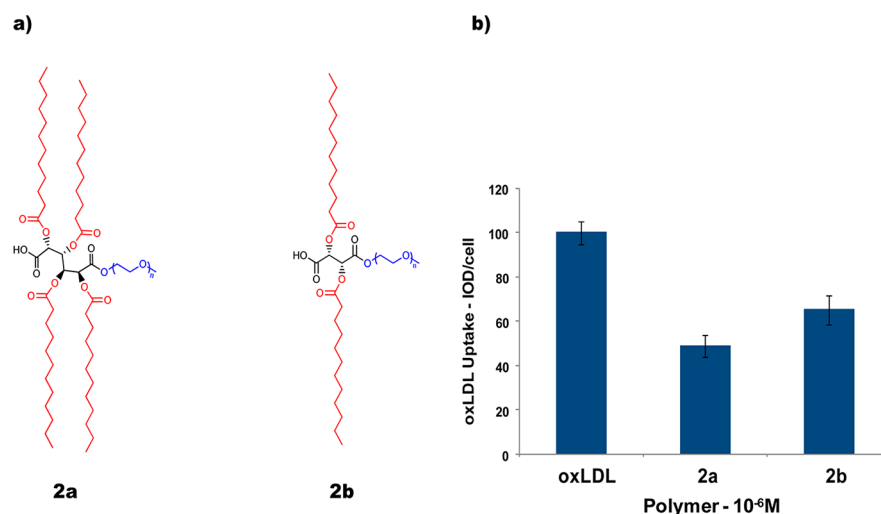


Figure 1. (a) Chemical structures of nanoscale AMs bearing four and two aliphatic arms, respectively. (b) AM inhibition of oxLDL in PBMC macrophages.

1b). Although these results suggest that lipophilicity impacts physicochemical and biological properties, it must be noted that the sugar backbones of **2a** and **2b** have different stereochemistries: mucic acid is a chiral, optically inactive, meso compound, and L-TA is chiral, but optically active. Studies performed by our research group and others have demonstrated that stereochemistry can greatly impact a polymer's physicochemical and biological properties.^{15b,19–21} Furthermore, because chirality influences numerous biological events/processes, stereoselective interactions between chiral materials and biological systems has been the topic of recent reviews.²² It is, therefore, possible that this disparity in the properties of **2a** and **2b** is a consequence of lipophilicity, stereochemistry, or both. Investigation into the contribution each factor makes to our AMs' biological activities would, therefore, aid our understanding of the scavenger receptor binding mechanism and enable our ability to optimize polymer design for atherosclerotic treatments.

Herein, we present the synthesis of novel nanoscale AMs comprised of an L-TA backbone that bears four aliphatic chains, with the goal of ascertaining the influence of lipophilicity on polymer properties. Preparation of these AMs is achieved in two manners: (1) growing dendrons from the hydroxyl groups of L-TA, thus incorporating branching onto the sugar backbone (i.e., dendronized) or (2) coupling two L-TA backbones to each other, yielding an AM with a disugar backbone (i.e., disugar). The physicochemical properties of these polymers are assessed as well as their ability to inhibit oxLDL uptake in PBMC macrophages. Additionally, a meso analog of (**2b**) was prepared (called **2l**) to determine the influence of stereochemistry on the AM properties.

2. MATERIALS AND METHODS

2.1. Materials. All reagents and solvents were purchased from Sigma-Aldrich and used as received unless otherwise noted. High-performance liquid chromatography (HPLC)-grade solvents were used unless otherwise noted. Monomethoxy-poly(ethylene glycol) (mPEG, Mn = 5000 Da) was azeotropically distilled with toluene prior to use. The following compounds were prepared as previously described: **2a**,¹³ **2b**,²³ and benzylidene-protected 2,2-bis-(hydroxymethyl)propionic acid (BP-BMPA).²⁴ (**2l**), a structural analogue of **2b**, was also prepared using the same procedure as **2b**, but using meso-tartaric acid monohydrate. Prior to use, meso-tartaric

acid monohydrate was azeotropically distilled with toluene to remove water (3 × 50 mL) and dried under high vacuum for 4 h.

2.2. Instrumentation. ¹H NMR spectra were obtained using a Varian 400 or 500 MHz spectrophotometer with TMS as the internal reference. Samples were dissolved in CDCl₃, or CDCl₃ with a few drops of DMSO-*d*₆ if necessary. IR spectra were recorded on a ThermoScientific Nicolet is10 series spectrophotometer using OMNIC software by solvent-casting samples on a salt plate. Mass spectrometry was done on ThermoQuest Finnigan LCQ-DUO system that includes a syringe pump, an optional divert/inject valve, an atmospheric pressure ionization (API) source, a mass spectrometer (MS) detector, and the Xcalibur data system. Samples were prepared at a concentration of 10 μg/mL in HPLC-grade CH₂Cl₂. Molecular weights (MW) were determined using size exclusion chromatography (SEC) with respect to PEG standards (Sigma-Aldrich) on a Waters Strygel HR 3 THF column (7.8 × 300 mm). The Waters LC system (Milford, MA) was equipped with a 2414 refractive index detector, a 1515 isocratic HPLC pump, and 717plus autosampler. Samples (10 mg/mL) were dissolved in THF and filtered using 0.45 μm pore size nylon or PTFE syringe filters (Fisher Scientific). Dynamic light scattering (DLS) analysis was carried out on a Zetasizer nanoseries ZS90 (Malvern instruments) in triplicate. CMC studies were carried out on a Spex fluoromax-3 spectrofluorometer (Jobin Yvon Horiba) at 25 °C in triplicate.

2.3. Synthesis. 2.3.1. Synthesis of 2c. **2c** was prepared in the same manner as the previously synthesized **0cM**,²⁵ using **2b** (1.06 g, 0.19 mmol), *N*-hydroxysuccinimide (NHS) (0.09 g, 0.77 mmol), and *N'*-dicyclohexylcarbodiimide (DCC) (1 M in DCM) (0.31 mL) to yield **2c** as a white powder (0.92 g, 85%). ¹H NMR (CDCl₃): δ = 0.86 (t, 6), 1.26 (m, 32), 1.60 (b, 4), 2.39 (b, 4), 2.90 (s, 4), 3.41 (m, ~400), 5.66 (s, 2); M_w = 5.5 kDa; PDI = 1.07.

2.3.2. Synthesis of 2d. **2d** was prepared similar to the previously prepared **1N**,²⁶ using **2c** (0.51 g, 0.09 mmol), propylamine (48.7 μL, 0.73 mmol), and triethylamine (NET₃) (197.4 μL, 1.42 mmol) to yield **2d** as a white powder (0.42 g, 82%). ¹H NMR (CDCl₃): δ = 0.85 (t, 6), 1.21 (m, 32), 1.58 (b, 4), 2.28 (b, 4), 3.38 (s, 2), 3.41 (m, ~400), 4.42 (s, 2), 5.30 (s, 1), 5.74 (s, 1); M_w = 5.6 kDa; PDI = 1.06.

2.3.3. Synthesis of 2e. Lauryl-acylated tartaric acid²³ (0.30 g, 0.59 mmol) and NHS (0.27 g, 2.36 mmol) were weighed into a round-bottom flask and placed under Ar(g). Anhydrous dichloromethane (DCM) and 6 mL of anhydrous dimethyl formamide (DMF) were then added to the round-bottom flask to dissolve the reagents. 1.48 mL DCC (1 M in DCM) was added dropwise to the reaction flask over 1 h via syringe pump. The reaction mixture was stirred at room temperature under argon for 24 h, cooled, and the resulting white solid precipitate (dicyclohexylurea) was removed by vacuum filtration. The filtrate was washed with 0.1 N HCl (20 mL), followed by 50:50

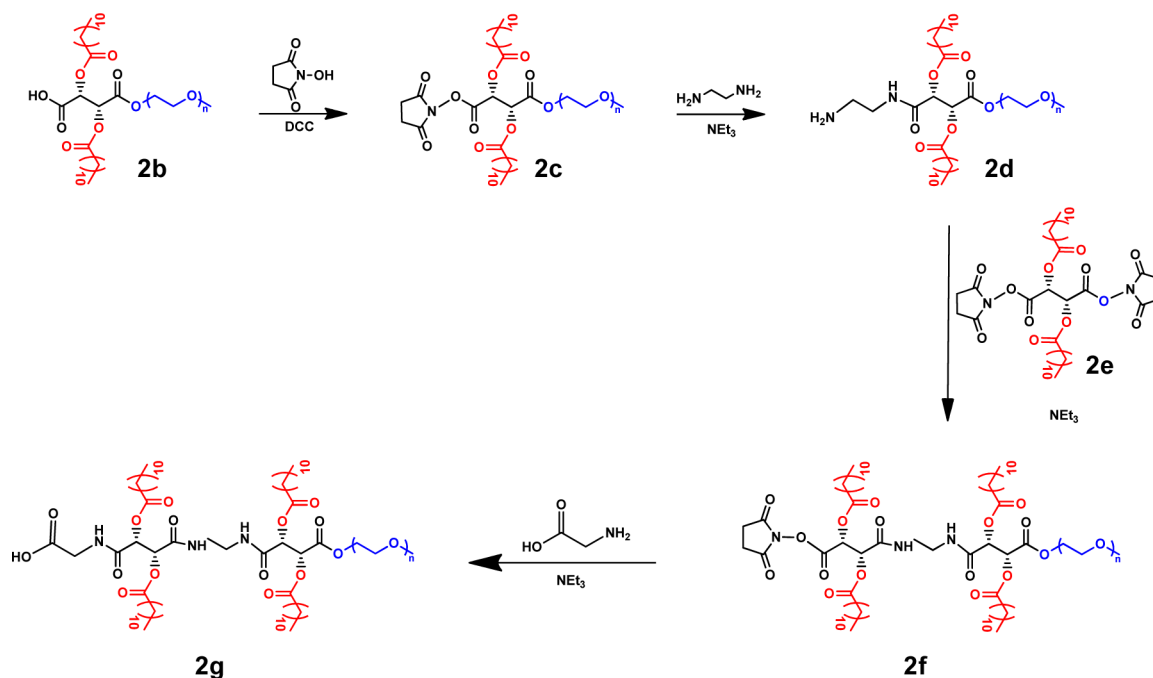


Figure 2. Synthetic scheme for linear disugar AM, 2g.

brine:water (2 × 20 mL), dried over MgSO₄, and concentrated via rotary evaporation. The product was precipitated from hexanes yielding 2e as a white solid (0.42 g, 29%). IR (cm⁻¹, thin film from CHCl₃): 1831, 1745. ¹H NMR (CDCl₃): δ = 0.87 (t, 6), 1.26 (m, 32), 1.65 (m, 4), 2.48 (t, 4), 2.83 (s, 8), 6.23 (s, 2). ¹³C NMR (CDCl₃): 14.34, 22.91, 24.58, 25.73, 29.46, 29.57, 29.68, 29.85, 32.14, 33.50, 68.61, 161.75, 167.98, 172.18. [M + NH₄]⁺_{theo} = 726.9, GC-MS: [M + NH₄]⁺_{calc} = 726.1.

2.3.4. Synthesis of 2f. 2d (0.12 g, 0.02 mmol) was added to a round-bottom flask and dissolved in 5 mL of anhydrous DCM and 5 mL of anhydrous DMF. After the addition of NEt₃ (50 μL, 0.36 mmol), the reaction mixture was allowed to stir under Ar(g). 2e (0.015 g, 0.02 mmol) was dissolved in DCM (5 mL) and added dropwise to the reaction flask via syringe pump at a rate of 1 mL/h. Upon complete 2e addition, the reaction was allowed to stir at room temperature under argon for 24 h. The reaction was filtered to remove insoluble triethylamine salts. The filtrate was washed with 0.1 N HCl (20 mL), followed by 50:50 brine:water (2 × 20 mL), dried over MgSO₄, and concentrated via rotary evaporation. The product was precipitated from diethyl ether yielding 2f as a white solid (0.097 g, 75%). ¹H NMR (CDCl₃): δ = 0.87 (t, 12), 1.21 (m, 64), 1.59 (b, 8), 2.38 (b, 8), 2.90 (s, 4), 3.41 (m, ~400), 5.30 (s, 1), 5.74 (s, 1); M_w = 6.3 kDa; PDI = 1.07.

2.3.5. Synthesis of 2g. Glycine (0.0015 g, 0.02 mmol) was added to a round-bottom flask and dissolved in anhydrous DCM (5 mL) and anhydrous DMF (5 mL). Upon addition of NEt₃ (10 μL, 0.07 mmol), the reaction mixture was allowed to stir under Ar(g). 2f (0.03 g, 0.005 mmol) was dissolved in 5 mL DCM and added dropwise to the reaction flask via syringe pump at a rate of 1 mL/h. Upon complete 2e addition, the reaction was allowed to stir at room temperature under argon for 24 h. The reaction was filtered to remove insoluble triethylamine salts. The filtrate was washed with 0.1 N HCl (20 mL), followed by 50:50 brine:water (2 × 20 mL), dried over MgSO₄, and concentrated via rotary evaporation. The product was precipitated from diethyl ether yielding 2g as a white solid (0.01 g, 33%). ¹H NMR (CDCl₃): δ = 0.87 (t, 12), 1.21 (m, 64), 1.59 (b, 8), 2.38 (b, 8), 3.41 (m, ~400), 5.50 (s, 2); M_w = 6.3 kDa; PDI = 1.07.

2.3.6. Synthesis of 2h. 2h was prepared using an established literature procedure²⁴ using dibenzyl-L-tartrate (0.33 g, 0.99 mmol), BP-BMPA anhydride (1.05 g, 2.46 mmol), and 4-dimethylaminopyridine (DMAP) (0.06 g, 0.49 mmol), yielding 2h as light yellow crystals

(0.67 g, 92%). IR (cm⁻¹, thin film from CHCl₃): 3458, 3328, 1736. ¹H NMR (CDCl₃): δ = 1.01 (s, 6), 3.59 (dd, 4), 4.58 (dd, 4), 4.72 (d, 2), 5.02 (d, 2), 5.44 (s, 2), 5.84 (s, 2), 7.25 (m, 20). ¹³C NMR (CDCl₃): 17.76, 42.91, 68.21, 71.42, 73.22, 73.73, 101.99, 126.54, 128.25, 128.30, 128.66, 134.85, 138.04, 165.45, 172.62.

2.3.7. Synthesis of 2i. (2i) was prepared using an established literature procedure,²⁴ using 2h (0.65 g) 10% w/w Pd/C, HPLC grade DCM (15 mL), and HPLC grade methanol (15 mL), yielding 2i as white crystals (0.31 g, 97%). IR (cm⁻¹, thin film from THF): 3408 (br), 1742. ¹H NMR (CDCl₃): δ = 1.01 (s, 6), 3.52 (m, 8), 5.39 (s, 2). ¹³C NMR (CDCl₃): 17.76, 42.91, 68.21, 71.42, 73.22, 73.73, 165.45, 172.62.

2.3.8. Synthesis of 2j. 2i (0.36 g, 0.95 mmol), lauroyl chloride (1.1 mL, 4.76 mmol), and zinc chloride (0.04 g, 0.30 mmol) were added to a round-bottom flask. Anhydrous DCM (2 mL) was added, and the reaction was stirred at room temperature under argon for 24 h. Water (5 mL) and diethyl ether (10 mL) were added to quench the reaction. After stirring for 1 h, the reaction mixture was diluted with diethyl ether (20 mL) and washed with water (5 × 20 mL), dried over MgSO₄, and concentrated via rotary evaporation. The product was precipitated from cold hexanes (refrigerated for 2 days) yielding 2j as white crystals (0.34 g, 32%). IR (cm⁻¹, thin film from CH₂Cl₂): 3514, 1746. ¹H NMR (CDCl₃): δ = 0.86 (t, 12), 1.26 (m, 70), 1.59 (b, 8), 2.29 (t, 8), 4.16 (m, 8), 5.62 (s, 2). ¹³C NMR (CDCl₃): 13.08, 17.79, 21.67, 23.58, 23.68, 27.90, 28.05, 28.13, 28.16, 28.23, 28.32, 28.36, 28.38, 28.43, 28.55, 28.57, 30.89, 32.12, 32.31, 42.91, 68.21, 71.42, 73.22, 73.73, 165.45, 168.12. [M - 2H]⁻_{theo} = 1109.1, GC-MS: [M - 2H]⁻ = 1109.2.

2.3.9. Synthesis of 2k. 2k was prepared using an established literature procedure,¹³ using 2j (0.20 g, 1.8 mmol), mPEG (0.28 g, 0.06 mmol), DCC (0.19 mL, 1.9 mmol), and 4-(dimethylamino)-pyridinium p-toluene-sulfonate (DPTS) (0.02 g, 0.007 mmol) to yield 2k as a white powder (0.29 g, 85%). ¹H NMR (CDCl₃): δ = 0.88 (t, 12), 1.30 (m, 70), 1.61 (b, 8), 2.29 (t, 8), 3.63 (m, ~400H), 4.18 (m, 8), 5.5 (s, 1), 5.7 (s, 1); M_w = 6.3 kDa; PDI = 1.15.

2.4. CMC Measurements. A solution of pyrene, a fluorescence probe molecule, was made up to a concentration of 5 × 10⁻⁶ M in acetone. Samples were prepared by adding 1 mL of pyrene solution to a series of vials and allowing the acetone to evaporate. AMs were dissolved in HPLC-grade water and diluted to a series of concentrations from 1 × 10⁻³ M to 1 × 10⁻¹⁰ M. AM-pyrene

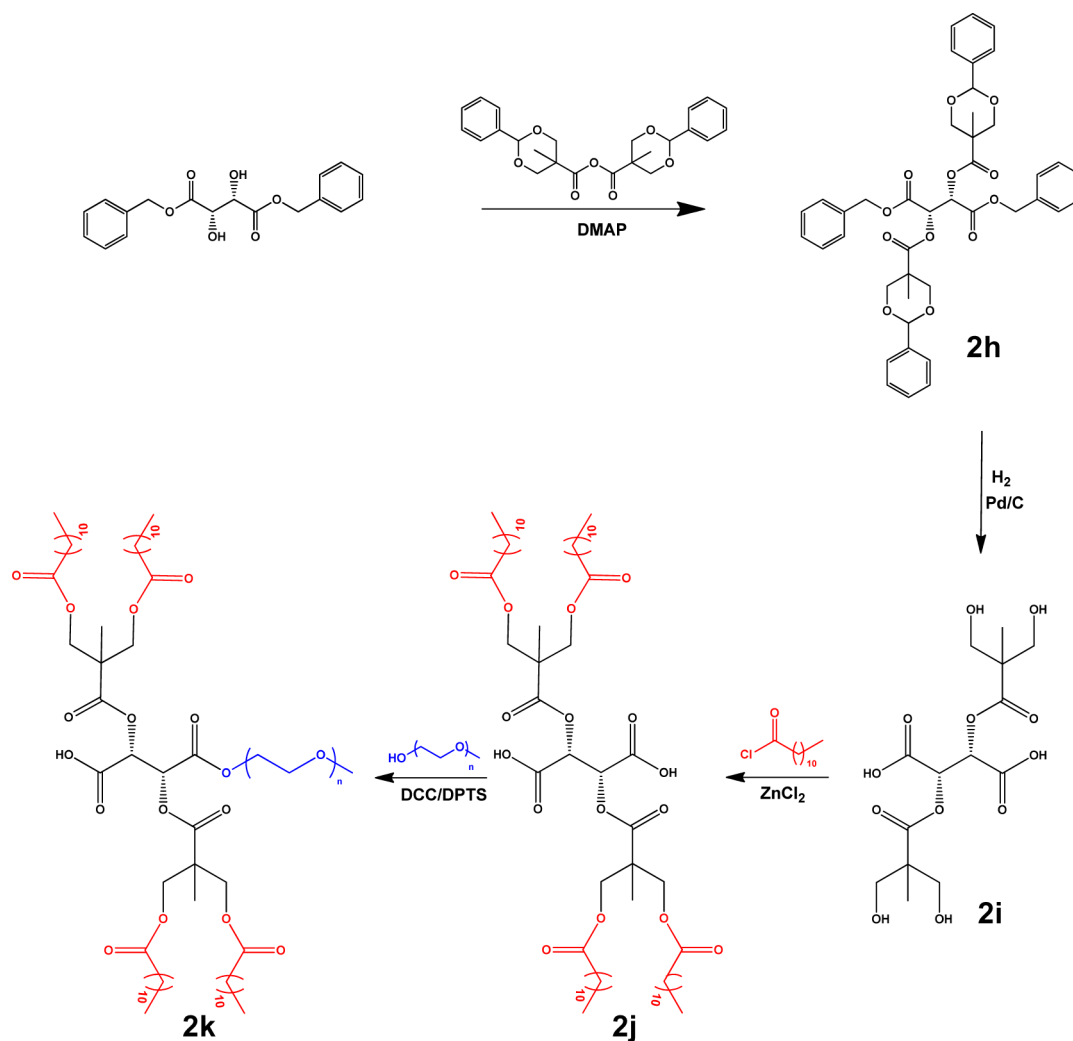


Figure 3. Synthetic scheme for dendronized AM, 2k.

solutions (10 mL) were shaken overnight at 37 °C to allow partition of the pyrene into the micelles. The concentration of pyrene in all samples was 5×10^{-7} M. Emission was performed from 300 to 360 nm, with 390 nm as the excitation wavelength. The maximum absorption of pyrene shifted from 332 to 334.5 nm on micelle formation.²⁷ The ratio of absorption of encapsulated pyrene (334.5 nm) to pyrene in water (332 nm) was plotted as the logarithm of polymer concentrations. The inflection point of the curve was taken as the CMC.

2.5. ClogP Calculations. ClogP values were derived using the CambridgeSoft ChemDraw software. The calculated values were of the AM hydrophobic domain as the PEG component was constant for all polymers.

2.6. Cell Culture. PBMCs were isolated from human buffy coats (Blood Center of New Jersey; East Orange, NJ) by centrifugation through Ficoll-Paque density gradient (GE Healthcare). PBMCs were plated into T-175 flasks, and monocytes were selected via plastic adherence by washing thrice with phosphate buffered saline (PBS) after 24 h. Monocytes were cultured for 7 days in RPMI 1640 (ATCC) supplemented with 10% fetal bovine serum (FBS), 1% penicillin/streptomycin, and 50 ng/mL M-CSF (macrophage colony-stimulating factor) for differentiation into macrophages.

2.7. oxLDL Oxidation. PBMC-derived macrophages were cocultured with 10 μ g/mL of 3,3'-dioctadecyloxycarbocyanine (DiO) labeled oxLDL (Kalen Biomedical) and nanolipoblocker (NLB) micelles (10^{-5} to 10^{-7} M) for 24 h in serum-free RPMI 1640. Cells were then fixed with 4% paraformaldehyde and counterstained with Hoechst 33342 prior to epifluorescent imaging using a Nikon Eclipse

TE2000-S. oxLDL uptake was quantified using ImageJ and normalized to conditions receiving no polymer treatment.

2.8. Statistical Analysis. Each in vitro experiment was performed at least twice, and three replicate samples were investigated in each experiment. Five images per well were captured and analyzed. The results were then evaluated using analysis of variance (ANOVA). Significance criteria assumed a 95% confidence level ($P < 0.05$). Standard error of the mean is reported in the form of error bars on the graphs of the final data.

3. RESULTS AND DISCUSSION

Preparation of novel nanoscale AMs based on L-TA and bearing four aliphatic chains was achieved via two synthetic methods: (1) coupling two L-TA backbones, yielding an AM with a linear backbone (referred to as “linear disugar” in this paper); and (2) incorporating branch points by growing dendrons from the L-TA hydroxyl groups (referred to as “dendronized”). The linear disugar AM was prepared by esterification of the previously synthesized 2b²³ with NHS to yield 2c. The NHS group was subsequently displaced by ethylene diamine to form the amine-terminated AM, 2d. Coupling of this polymer to a di-NHS, lauryl-acylated L-TA (2e) yielded the NHS-capped linear disugar, 2f. Amidation using glycine rendered the carboxylic acid-terminated disugar, 2g, as the final product (Figure 2). Polymers prepared at each step in the synthesis were characterized via ¹H NMR and SEC.

The synthesis of the dendronized AM was based on a divergent synthesis using an anhydride coupling developed by Ihre et al.²⁴ (Figure 3). Dibenzyl-L-tartrate was coupled with the previously reported benzylidene-protected BP-BMPA anhydride using DMAP as the acylating catalyst to afford **2h** at a 92% yield. The benzylidene protecting groups as well as the benzyl esters were removed by catalytic hydrogenolysis using H₂(g) and 10% w/w Pd/C as catalyst. Upon removal of catalyst by filtration, the deprotection rendered L-TA with four terminal hydroxyl groups (**2i**) in near quantitative yields. Using the dendronized L-TA, the corresponding AM was synthesized by modifying a previously published method for the preparation of **2a**, which has a mucic acid backbone.¹³ Briefly, the two-step procedure involves acylating **2i** with lauroyl groups followed by coupling to PEG. During the initial acylation step, some modifications were required when **2i** was used in place of mucic acid. For example, to achieve an acceptable yield (40%) of **2j**, the number of equivalents of acylating agent (lauroyl chloride) was significantly reduced from 15 (with mucic acid) to 5 (with dendronized L-TA), as isolation and purification proved problematic with a large excess of lauroyl chloride. It was also necessary that the reaction occur at room temperature and in solvent (DCM). Coupling of the PEG and **2j** using DCC as the coupling agent and DPTS as the catalyst proceeded as reported, yielding the dendritic AM, **2k**, in 85% yield. The resultant polymer was characterized via SEC and ¹H NMR.

With these unique AMs, the impact of hydrophobicity on the physicochemical properties, namely, hydrodynamic radius and CMC, was evaluated. CMC values were measured using a previously reported fluorimetry technique using pyrene as the fluorescence probe.^{27a} The linear disugar AM, **2g**, formed micelles of ~117 nm in diameter while the dendronized AM, **2k**, formed ~17 nm micelles. The larger micelles formed by **2g** may be attributed to the increased length of the hydrophobic core, a consequence of tethering two L-TA sugars. A similar trend was observed by Zeng and Pitt²⁸ who, when preparing the amphiphilic copolymer poly(ethylene oxide)-*b*-poly(*N*-isopropylacrylamide(*N*IPAAm)-*co*-2-hydroxyethyl methacrylate-lactate,_n), observed that lengthening of the hydrophobic poly(*N*IPAAm) block resulted in larger micelles. Both AMs exhibited ClogP values (**2g**: 17.36, **2k**: 21.00; see Table 1)

Table 1. Physicochemical Properties of AMs^a

polymer	size (nm) ^b	CMC (M)	ClogP
2a	20	1.20 × 10 ⁻⁷	20.37
2b	7	1.25 × 10 ⁻⁵	9.09
2g	117	1.58 × 10 ⁻⁵	17.38
2k	17	5.84 × 10 ⁻⁵	21.00
2l	8	6.12 × 10 ⁻⁶	9.09

^aThe hydrodynamic size and critical micelle concentrations were experimentally measured; the hydrophobicity coefficient was estimated for the non-PEG components of AMs. ^bZ-average size.

similar to that of their four-arm, mucic acid-based analogue, **2a** (20.37). These results suggest that micelle size is influenced by the number of hydrophobic arms as well as by the length of the hydrophobic domain, i.e., overall lipophilicity. In regards to micelle assembly, both **2g** and **2k** have CMC values on the order of 10⁻⁵ M, similar to that of **2b**. Each of these polymers possess an L-TA backbone, which suggests that the stereochemistry of the hydrophobic core plays a key role in micelle

self-assembly, an observation also made by Makino et al. in their study of the in vivo blood clearance of lactosomes.²⁹

The new AMs were then assessed for their ability to inhibit oxLDL internalization in PBMC macrophages (Figure 4). In

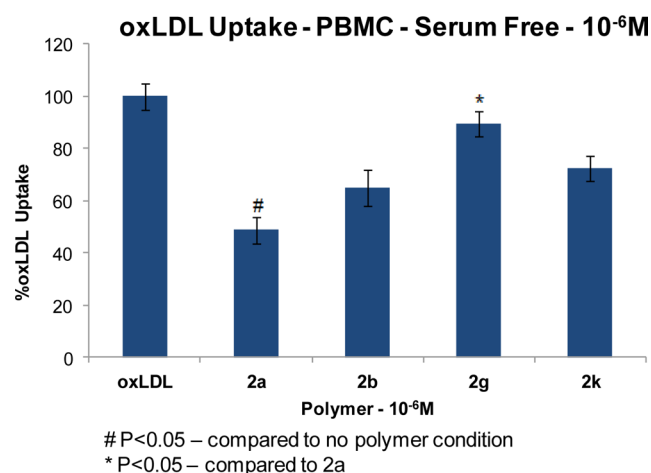


Figure 4. Role of AMs with varying hydrophobicity on the in vitro inhibition of oxLDL uptake in PBMC macrophages.

vitro experiments were carried out by incubating the cells with 10⁻⁶ M polymers and fluorescently labeled oxLDL for 24 h at 37 °C. As a control, the basal uptake of oxLDL when no polymer was present was evaluated. The previously synthesized **2a**¹³ and **2b**²² were compared to the newly synthesized polymers. Based on the improved inhibition of oxLDL internalization of **2a** (52%) relative to **2b** (35%), it was anticipated that increasing the overall hydrophobicity of the L-TA based polymers would result in decreased oxLDL internalization. The converse, however, was observed: both **2g** and **2k** were far less efficacious in inhibiting oxLDL uptake (11% and 27% inhibition, respectively). This result suggests that just the extrinsic hydrophobicity of AMs does not uniquely govern blockage of macrophage oxLDL uptake mechanisms, but that other factors likely contribute to **2a**'s improved efficacy of oxLDL inhibition.

Because **2a** and **2b** differ not only in their overall lipophilicity, but also in stereochemistry, we probed the influence of stereochemistry on AM physicochemical and biological properties. A new AM was prepared, **2l** (Figure 5a), to be structurally analogous to **2b** while being stereochemically analogous to **2a**. Analysis of the solution behavior of **2l** revealed micelles that were similar in size (~8 nm) to **2b**, but more stable (CMC values of 10⁻⁶ M as opposed to 10⁻⁵ M) under physiological conditions. These findings correlate well with the results above: the number of hydrophobic arms and the length of the hydrophobic domain influence micelle size, while stereochemistry influences the solution stability of micelles. Recently, our research group performed a study comparing the oxLDL inhibition of **2a** to a structurally analogous, but stereochemically different AM based on saccharic acid.^{15b} Although the AMs differed by only one stereocenter in the hydrophobic domain, their ability to inhibit oxLDL internalization was vastly different with **2a** showing 60% inhibition compared to 10% inhibition by the saccharic acid-based polymer. Based on this earlier work, it was anticipated that AMs based on L- and meso-tartaric acid (**2b** and **2l**, respectively) would also have markedly different biological

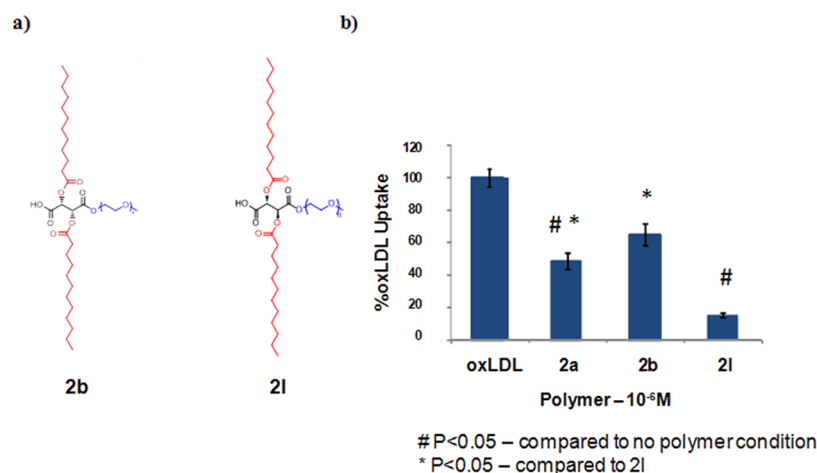


Figure 5. (a) Chemical structure of AM bearing two aliphatic arms (**2b**) and an equivalent AM with meso stereochemistry (**2l**). (b) Effect of stereochemistry on the in vitro inhibition of oxLDL uptake in PBMC macrophages.

properties. Additionally, it was hypothesized that if stereochemistry is a major contributor to polymer-scavenger receptor binding, then the ability of **2l** to inhibit oxLDL uptake should be similar to the stereochemically analogous **2a**. The results of this current study confirmed that minute changes, such as altering one stereocenter along the polymer's sugar backbone, greatly affects oxLDL uptake and also revealed **2l** as a better inhibitor to oxLDL uptake than the "gold standard", **2a**. Although it has less overall lipophilicity relative to **2a**, **2l** showed the highest degree of inhibition of oxLDL internalization, 89% (Figure 5b). This result further demonstrates that overall AM lipophilicity may not be the most critical factor in governing oxLDL inhibition, but rather, stereochemistry of the hydrophobic domain could dramatically influence the polymer-blockage of oxLDL uptake.

4. CONCLUSIONS

Innovative nanoscale AMs were designed to investigate the influence of hydrophobicity and stereochemistry on physicochemical and biological properties. Solution aggregation studies indicate that micellar size is governed both by the number of hydrophobic arms and the length of the hydrophobic domain, whereas micelle stability is governed by the stereochemistry. In vitro experiments evaluating oxLDL inhibition displayed similar results: stereochemistry (not lipophilicity) of hydrophobic domain has a significant impact on oxLDL internalization. Thus for polymers with equivalent levels of hydrophobicity, the nature of the AM stereochemistry appears to be a critical parameter for modulating the antiatherogenic activity of polymers. These insights could be relevant to the design of polymer therapeutics for the treatment of cardiovascular disease.

AUTHOR INFORMATION

Corresponding Author

*Tel: 732-445-0361; Fax: 732-445-7036; E-mail: keuhrich@rutgers.edu.

Notes

The authors declare no competing financial interest.

ACKNOWLEDGMENTS

This study was supported by NIH grants (R21093753 to P.V.M. and NIH grant R01 HL107913 to P.V.M. and K.E.U.).

The authors thank Li Gu for assistance with critical micelle concentration measurements.

REFERENCES

- (1) Li, A. C.; Glass, C. K. *Nat. Med.* **2002**, *8*, 1235–1242.
- (2) Yoshimoto, T.; Takahashi, Y.; Kinoshita, T.; Sakashita, T.; Inoue, H.; Tanabe, T. *Adv. Exp. Med. Biol.* **2002**, *507*, 403–407.
- (3) Goldstein, J. L.; Ho, Y. K.; Basu, S. K.; Brown, M. S. *Proc. Natl. Acad. Sci. U.S.A.* **1979**, *76*, 333–337.
- (4) Podrez, E. A.; Febbraio, M.; Sheibani, N.; Schmitt, D.; Silverstein, R. L.; Hajjar, D. P.; Cohen, P. A.; Frazier, W. A.; Hoff, H. F.; Hazen, S. L. *J. Clin. Invest.* **2000**, *105*, 1095–1108.
- (5) de Winther, M. P.; van Dijk, K. W.; Havekes, L. M.; Hofker, M. H. *Arterioscler., Thromb., Vasc. Biol.* **2000**, *20*, 290–297.
- (6) Brown, M. S.; Goldstein, J. L. *Annu. Rev. Biochem.* **1983**, *52*, 223–261.
- (7) Steinberg, D. *J. Biol. Chem.* **1997**, *272*, 20963–20966.
- (8) Boullier, A.; Friedman, P.; Harkewicz, R.; Hartvigsen, K.; Green, S. R.; Almazan, F.; Dennis, E. A.; Steinberg, D.; Witztum, J. L.; Quehenberger, O. *J. Lipid Res.* **2005**, *46*, 969–976.
- (9) Yoshiizumi, K.; Nakajima, F.; Dobashi, R.; Nishimura, N.; Ikeda, S. *Bioorg. Med. Chem. Lett.* **2004**, *14*, 2791–2795.
- (10) Guaderrama-Diaz, M.; Solis, C. F.; Velasco-Loyden, G.; Lacleite, J.; Mas-Oliva, J. *Mol. Cell. Biochem.* **2005**, *271*, 123–132.
- (11) Broz, P.; Benito, S. M.; Saw, C.; Burger, P.; Heider, H.; Pfisterer, M.; Marsch, S.; Meier, W.; Hunziker, P. *J. Controlled Release* **2005**, *102*, 475–488.
- (12) Chnari, E.; Nikitczuk, J. S.; Wang, J. Z.; Uhrich, K. E.; Moghe, P. V. *Biomacromolecules* **2006**, *7*, 1796–1805.
- (13) Tian, L.; Yam, L.; Zhou, N.; Tat, H.; Uhrich, K. E. *Macromolecules* **2004**, *370*, 538–543.
- (14) Iverson, N. M.; Sparks, S. M.; Demirdirek, B.; Uhrich, K. E.; Moghe, P. V. *Acta Biomaterialia* **2010**, *6*, 3081–3091.
- (15) (a) York, A. W.; Zablocki, K. R.; Lewis, D. R.; Gu, L.; Uhrich, K. E.; Prud'homme, R. K.; Moghe, P. V. *Adv. Mater.* **2012**, *24*, 733–739. (b) Hehir, S.; Plourde, N. M.; Gu, L.; Poree, D. E.; Welsh, W. J.; Moghe, P. V.; Uhrich, K. E. *Acta Biomater.* **2012**, *8*, 3956–3962. (c) Plourde, N. M.; Kortagere, S.; Welsh, W.; Moghe, P. V. *Biomacromolecules* **2009**, *10*, 1381–1391. (d) Chnari, E.; Nikitczuk, J. S.; Wang, J.; Uhrich, K. E.; Moghe, P. V. *Biomacromolecules* **2006**, *7*, 1796–1805.
- (16) Petit, F.; Audebert, R.; Iliopoulos, I. *Colloid Polym. Sci.* **1995**, *273*, 777–781.
- (17) Porcar, I.; Cottet, H.; Gareil, P.; Tribet, C. *Macromolecules* **1999**, *32*, 3922–3929.
- (18) Gao, J. Y.; Dubin, P. L. *Biopolymers* **1999**, *49*, 185–193.

- (19) Reeve, M. S.; McCarthy, S. P.; Downey, M. J.; Gross, R. A. *Macromolecules* **1994**, *27*, 825–831.
- (20) Sun, T.; Han, D.; Riehemann, K.; Chi, L.; Fuchs, H. S. *J. Am. Chem. Soc.* **2007**, *129*, 1496–1497.
- (21) (a) Wang, X.; Gan, H.; Sun, T. L.; Su, B. L.; Fuchs, H.; Vestweber, D.; Butz, S. *Soft Matter* **2010**, *6*, 3851–3855. (b) Wang, X. G., H.; Sun, T. *Adv. Funct. Mater.* **2011**, *21*, 3276–3281.
- (22) (a) Sun, T. L.; Qing, G. Y.; Su, B. L.; Jiang, L. *Chem. Soc. Rev.* **2011**, *40*, 2909–2921. (b) Zhang, M. X.; Qing, G. Y.; Sun, T. L. *Chem. Soc. Rev.* **2012**, *41*, 1972–1984. (c) Qing, G.; Sun, T. *NPG Asia Mater.* **2012**, *4*, 1–13.
- (23) Tao, L.; Urrich, K. E. *J. Colloid Interface Sci.* **2006**, *298*, 102–110.
- (24) Ihre, H.; Padilla de Jesus, O. L.; Frechet, J. M. J. *J. Am. Chem. Soc.* **2001**, *123*, 5907–5917.
- (25) Djordjevic, J.; Del Rosario, L. S.; Wang, J. Z.; Urrich, K. E. *J. Bioact. Compat. Polym.* **2008**, *23*, 532–551.
- (26) Sparks, S. M.; Waite, C. L.; Harmon, A. M.; Nusblat, L. M.; Roth, C. M.; Urrich, K. E. *Macromol. Biosci.* **2011**, *11*, 1192–1200.
- (27) (a) Astafieva, I.; Zhong, X. F.; Eisenberg, A. *Macromolecules* **1993**, *26*, 7339–7352. (b) Meng, F. B.; Zhang, B. Y.; Lian, J.; Wu, Y. P.; Li, X. Z.; Yao, D. S. *J. Appl. Polym. Sci.* **2009**, *114*, 2195–2203. (c) Kalyanasundaram, K.; Thomas, J. K. *J. Am. Chem. Soc.* **1977**, *99* (7), 2039–2044.
- (28) Zeng, Y.; Pitt, W. G. *J. Biomater. Sci., Polym. Ed.* **2006**, *17*, 591–604.
- (29) Makino, A.; Hara, E.; Hara, I.; Yamahara, R.; Kurihara, K.; Ozeki, E.; Yamamoto, F.; Kimura, S. *J. Controlled Release* **2012**, *161*, 821–825.